

1991

# Raman Scattering and Lattice-Dynamical Calculations of Alkali-Metal Sulfates

D. Liu

*University of Nebraska - Lincoln*

H. M. Lu

*University of Nebraska - Lincoln*

John R. Hardy

*University of Nebraska - Lincoln*

F. G. Ullman

*University of Nebraska - Lincoln*

Follow this and additional works at: <http://digitalcommons.unl.edu/physicshardy>



Part of the [Physics Commons](#)

---

Liu, D.; Lu, H. M.; Hardy, John R.; and Ullman, F. G., "Raman Scattering and Lattice-Dynamical Calculations of Alkali-Metal Sulfates" (1991). *John R. Hardy Papers*. 50.

<http://digitalcommons.unl.edu/physicshardy/50>

This Article is brought to you for free and open access by the Research Papers in Physics and Astronomy at DigitalCommons@University of Nebraska - Lincoln. It has been accepted for inclusion in John R. Hardy Papers by an authorized administrator of DigitalCommons@University of Nebraska - Lincoln.

Phys. Rev. B 44, 7387 - 7393 (1991)

# Raman scattering and lattice-dynamical calculations of alkali-metal sulfates

D. Liu, H. M. Lu, and J. R. Hardy

*Behlen Laboratory of Physics and the Center for Electro-Optics, University of Nebraska–Lincoln, Lincoln, Nebraska 68588*

F. G. Ullman

*Department of Electrical Engineering and Behlen Laboratory of Physics, University of Nebraska–Lincoln, Lincoln, Nebraska 68588*

Abstract

Raman-scattering measurements on single crystals of  $K_2SO_4$ ,  $Rb_2SO_4$ , and  $Cs_2SO_4$  have been made at both room and liquid-nitrogen temperatures. Lattice-dynamical calculations, based on a rigid-ion model using the Gordon-Kim method to calculate the short-range potentials, were performed. The influence of the alkali-metal ions on the lattice-dynamical properties of the crystals is discussed.

©1991 The American Physical Society. Used by permission.

URL: <http://link.aps.org/doi/10.1103/PhysRevB.44.7387>

DOI: 10.1103/PhysRevB.44.7387

## Raman scattering and lattice-dynamical calculations of alkali-metal sulfates

D. Liu, H. M. Lu, and J. R. Hardy

*Behlen Laboratory of Physics and the Center for Electro-Optics, University of Nebraska-Lincoln,  
Lincoln, Nebraska 68588*

F. G. Ullman

*Department of Electrical Engineering and Behlen Laboratory of Physics, University of Nebraska-Lincoln,  
Lincoln, Nebraska 68588*

(Received 26 December 1990)

Raman-scattering measurements on single crystals of  $K_2SO_4$ ,  $Rb_2SO_4$ , and  $Cs_2SO_4$  have been made at both room and liquid-nitrogen temperatures. Lattice-dynamical calculations, based on a rigid-ion model using the Gordon-Kim method to calculate the short-range potentials, were performed. The influence of the alkali-metal ions on the lattice-dynamical properties of the crystals is discussed.

### I. INTRODUCTION

At room temperature  $M_2SO_4$  ( $M=K,Rb,Cs$ ) crystals belong to the orthorhombic symmetry group  $Pnam$ , with four molecular units per unit cell as shown in Fig. 1. This is usually called the  $\beta$ - $K_2SO_4$  structure. Not only alkali-metal sulfates, but a large number of other compounds with the general molecular formula  $A_2BX_4$  also have this structure. One very interesting property demonstrated by some of these compounds is the incommensurate phase transition that many of them exhibit. Typical of these, and also the most studied, is  $K_2SeO_4$ . However, in spite of their similarity in crystal structure to that of  $K_2SeO_4$ , the three alkali-metal sulfates  $M_2SO_4$  ( $M=K,Rb,Cs$ ) do not undergo any known incommensurate phase transitions. Thus a systematic and detailed study of these crystals for comparison with others among this isomorphous group could give further insight into the driving mechanism of these incommensurate phase transitions as well as provide information about the influence of the properties of specific ions on crystal lattice-dynamical properties.

The room temperature structure of the  $K_2SO_4$  crystal is  $Pnam$ .<sup>1</sup> At 860 K, it transforms into a hexagonal phase. A phase transition at 56 K was observed by Gesi, Tominaga, and Urabe<sup>2</sup> and was suggested to be not incommensurate.

The first complete Raman spectra of  $K_2SO_4$  were reported by Debeau<sup>3</sup> for room temperature. A Raman-scattering measurement on  $Cs_2SO_4$  at room temperature was made by Venkateswarlu and Broida.<sup>4</sup> Montero, Schmolz, and Haussuhl<sup>5</sup> measured the Raman spectra of  $K_2SO_4$ ,  $Rb_2SO_4$ ,  $Cs_2SO_4$ , and  $Tl_2SO_4$  at room temperature and of  $K_2SO_4$  and  $Tl_2SO_4$  at 80 K. They observed a linear relation between the internal mode frequencies and the electronegativities of the cations and that the variation of the frequencies of the external mode from crystal to crystal was well correlated to the masses of the cations. Scrocco<sup>6</sup> performed Raman measurements on  $K_2SO_4$  at 87 K and room temperature, but did not report complete

spectra.

In this paper we report the results of Raman-scattering measurements and lattice-dynamical calculations on the alkali-metal sulfate crystals  $K_2SO_4$ ,  $Rb_2SO_4$ , and  $Cs_2SO_4$ . The Raman measurements were performed at both room and liquid-nitrogen temperatures. Lattice-dynamical calculations were carried out for all three crystals. The calculations are based on a rigid-ion model using Gordon-Kim short-range pair potentials, which has recently been extended to molecular ionic crystals.<sup>7,8</sup> In Ref. 8 this method was used for lattice-dynamical calculations on  $K_2SO_4$  to pinpoint important differences in the lattice-dynamical properties between incommensurate  $K_2SeO_4$  and commensurate  $K_2SO_4$ . In this paper the calculations are extended to two other alkali-metal sulfates  $Rb_2SO_4$  and  $Cs_2SO_4$ . It is shown that the calculations successfully predict structure and dynamical differences among the three crystals that are in general agreement with the experimental results.

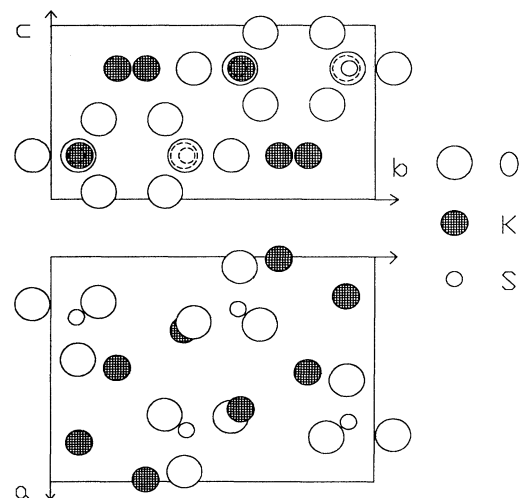


FIG. 1. Crystal structure of  $Pnam$   $K_2SO_4$ .

## II. EXPERIMENTAL PROCEDURES

Raman-scattering measurements were made with a Spectra Physics 2016 argon-ion laser. The 514.5-nm line was used throughout this experiment. The laser power incident on the sample was about 80 mW. The sample was mounted in an exchange-gas-coupled liquid-nitrogen cryostat with computer-controlled temperature to within 0.1 K, which enabled Raman measurements to be made from 78 K to room temperature. A Spex 1401 75-cm-focal-length,  $f/6.8$ , double monochromator, combined with a thermoelectrically cooled photomultiplier, was used to collect and detect the scattered light. The slit widths of the monochromator used give a resolution of about  $2.0 \text{ cm}^{-1}$ . The photon-counting time was about 10 s at each frequency, and the scanning was in steps of  $0.5 \text{ cm}^{-1}$ .

The crystals used were all grown from aqueous solution by evaporation at constant temperature or with slow cooling.  $\text{Rb}_2\text{SO}_4$  and  $\text{Cs}_2\text{SO}_4$  powders used for crystal growing were obtained from Aldrich Chemicals Company with purities of 99.9%.  $\text{K}_2\text{SO}_4$  powders were obtained from Fisher Scientific Company with a purity of 99%. The crystals were polished into rectangular prisms with the surfaces perpendicular to the crystal axes.

Buehler microcloth and  $0.05 \mu\text{m Al}_2\text{O}_3$  slurry were used for polishing. The directions of the crystal axes were identified with two polarizers. The orientations of the crystals were determined by comparing their Raman spectra with known results. The samples usually had dimensions of several millimeters in each direction.

## III. EXPERIMENTAL AND CALCULATION RESULTS

The measured Raman frequencies of the three alkali-metal sulfates are listed in Tables I–III, together with the calculated values. The Raman spectra of the three crystals at liquid-nitrogen temperature in the external mode region are plotted in Figs. 2–4. According to the factor group analysis,<sup>5</sup> the number of external modes should be  $7A_g$ ,  $7B_{1g}$ ,  $5B_{2g}$ , and  $5B_{3g}$ . All the  $A_g$  external modes were identified for all three crystals, as were the  $B_{2g}$  and  $B_{3g}$  external modes. There should be the same number of  $B_{1g}$  external modes as  $A_g$  external modes; however, not all could be identified. All of the internal modes of the three crystals were identified.

The details of the calculation method to treat molecular ionic crystals were given in Refs. 7 and 8. The basic concept is to give separate consideration to intramolecu-

TABLE I. Experimental and calculated Raman frequencies of  $\text{K}_2\text{SO}_4$  (in  $\text{cm}^{-1}$ ).

$A_g$		Calc.	$B_{1g}$		Calc.	
298 K	78 K		298 K	78 K		
50	52	58	90	92	109	
97	97	119		96	140	
	105	129	106	110	147	
110	113	141	115	117	169	
132	134	170			196	
	162	187			208	
164	172	220			225	
448	450	491	454	455	507	$\nu_2$ of $\text{SO}_4^{2-}$
618	617	681	620	620	687	$\nu_4$ of $\text{SO}_4^{2-}$
628	630	693	634	635	707	
985	989	1049				$\nu_1$ of $\text{SO}_4^{2-}$
1096	1099	1208	1112	1114	1219	$\nu_3$ of $\text{SO}_4^{2-}$
1148	1152	1220	1169	1171	1231	$\nu_3$ of $\text{SO}_4^{2-}$
$B_{2g}$		Calc.	$B_{3g}$		Calc.	
298 K	78 K		298 K	78 K		
	78	69	74	74	34	
107	107	105	96	94	73	
134	141	121	105	105	120	
	147	161		144	154	
159	165	199	142	148	180	
457	457	486	458	459	500	$\nu_2$ of $\text{SO}_4^{2-}$
622	623	684	622	622	691	$\nu_4$ of $\text{SO}_4^{2-}$
1111	1115	1214	1108	1112	1210	$\nu_3$ of $\text{SO}_4^{2-}$

lar and intermolecular interactions. The starting point is to perform electronic calculations for the whole molecular ion  $\text{SO}_4^{2-}$  in the present case, to obtain realistic electron charge distributions and effective ion charges that contain the effect of electronic covalency. These distributions are used to describe intermolecular interactions in the same spirit as the original Gordon-Kim electron-gas model. These calculations also provide a harmonic expansion of the total energy of the molecular ion, which is used to describe the intramolecular interactions. The electronic calculations were performed using the software package GAUSSIAN86.<sup>9</sup> The electron charge densities for the alkali-metal ions  $\text{K}^+$  and  $\text{Rb}^+$  are from Ref. 10, and that for  $\text{Cs}^+$  are calculated with the software of Liberman, Cromer, and Waber.<sup>11</sup> The effective ion charges used for the alkali-metal ion  $M^+$  was +1.0, and those for the oxygen and sulfur ions were obtained from the electronic calculation of the  $\text{SO}_4^{2-}$  group using the Mulliken population analysis method. The effective ion charge found for the oxygen ion was  $-0.9700$  and for the sulfur ion 1.8801.

First, the crystal under consideration was statically relaxed by minimizing both the total forces acting on each ion and the stresses to get a stable equilibrium structure.

Then the vibrational frequencies of the crystal were calculated for the relaxed structure. The calculated structure parameters for the three alkali-metal sulfate crystals are listed in Table IV. The calculated Raman frequencies are listed in Tables I–III with the experimental values.

#### IV. DISCUSSION

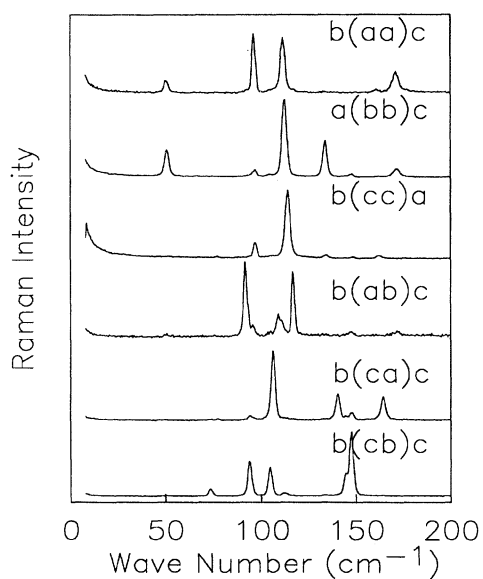
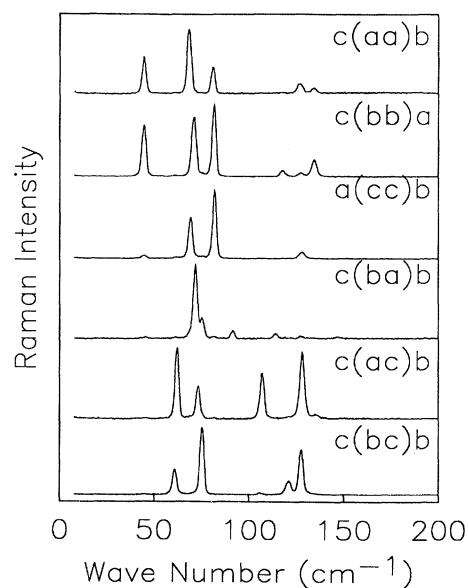
The three alkali-metal sulfates  $\text{K}_2\text{SO}_4$ ,  $\text{Rb}_2\text{SO}_4$ , and  $\text{Cs}_2\text{SO}_4$  have the same negative ion radical and have the same crystal structure. The only differences among the three crystals result from the properties of the positive metal ions. Different alkali-metal ions have different masses and different electronic structures. These factors, especially the electronic structure, have major influences on the lattice-dynamical properties of the crystals. Since all three alkali-metal ions have closed-shell electronic structures, the major differences in the electronic structure of the three alkali-metal ions can be well described by ionic radius, electronegativity, and the polarizability of the inner-shell electrons. The values of the masses, ionic radii, electronegativities, and the ionic polarizabilities are listed in Table V. It can be seen that the differences in ionic radii are larger than the differences in

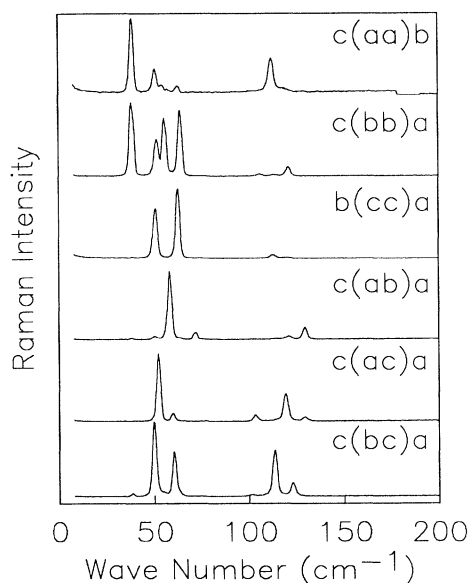
TABLE II. Experimental and calculated Raman frequencies of  $\text{Rb}_2\text{SO}_4$  (in  $\text{cm}^{-1}$ ).

$A_g$		Calc.	$B_{1g}$		Calc.	
298 K	78 K		298 K	78 K		
46	47	48	71	71	80	
69	70	87		75	104	
	76	95	92	92	115	
81	81	98	111	115	130	
115	118	136		147	141	
122	128	148			166	
128	136	172			176	
445	446	488	450	450	502	$\nu_2$ of $\text{SO}_4^{2-}$
613	613	677	617	617	684	$\nu_4$ of $\text{SO}_4^{2-}$
623	623	688	630	630	704	$\nu_4$ of $\text{SO}_4^{2-}$
977	980	1045				$\nu_1$ of $\text{SO}_4^{2-}$
1091	1093	1207	1103	1105	1218	$\nu_3$ of $\text{SO}_4^{2-}$
1132	1135	1218	1151	1154	1230	$\nu_3$ of $\text{SO}_4^{2-}$
$B_{2g}$		Calc.	$B_{3g}$		Calc.	
298 K	78 K		298 K	78 K		
65	64	64	63	63	48	
74	74	83	78	76	75	
108	108	99		106	90	
123	130	150	116	122	135	
	137	155	124	129	141	
454	454	485	455	455	496	$\nu_2$ of $\text{SO}_4^{2-}$
618	618	682	618	618	688	$\nu_4$ of $\text{SO}_4^{2-}$
1102	1104	1213	1100	1103	1208	$\nu_3$ of $\text{SO}_4^{2-}$

TABLE III. Experimental and calculated Raman frequencies of  $\text{Cs}_2\text{SO}_4$  (in  $\text{cm}^{-1}$ ).

$A_g$			$B_{1g}$			
298 K	78 K	Calc.	298 K	78 K	Calc.	
38	39	44	56	59	67	
48	51	67	70	72	79	
54	56	73	78	83	95	
62	64	78	124	130	98	
	107	125			125	
108	113	131			148	
114	120	147			159	
440	442	487	444	445	497	$\nu_2$ of $\text{SO}_4^{2-}$
608	609	676	612	611	681	$\nu_4$ of $\text{SO}_4^{2-}$
615	616	684	621	622	699	$\nu_4$ of $\text{SO}_4^{2-}$
970	970	1040				$\nu_1$ of $\text{SO}_4^{2-}$
1084	1084	1207	1092	1092	1217	$\nu_3$ of $\text{SO}_4^{2-}$
1119	1118	1216	1135	1136	1227	$\nu_3$ of $\text{SO}_4^{2-}$
$B_{2g}$			$B_{3g}$			
298 K	78 K	Calc.	298 K	78 K	Calc.	
49	52	59	49	52	48	
	60	69	60	60	71	
100	103	101	98	102	98	
112	120	134	109	114	119	
	129	143	118	124	129	
449	450	485	448	448	494	$\nu_2$ of $\text{SO}_4^{2-}$
613	614	679	612	612	684	$\nu_4$ of $\text{SO}_4^{2-}$
1091	1091	1213	1090	1090	1209	$\nu_3$ of $\text{SO}_4^{2-}$

FIG. 2. Raman spectra of  $\text{K}_2\text{SO}_4$  at 78 K.FIG. 3. Raman spectra of  $\text{Rb}_2\text{SO}_4$  at 78 K.

FIG. 4. Raman spectra of  $\text{Cs}_2\text{SO}_4$  at 78 K.

electronegativities, which are relatively quite small. The differences in ionic polarizabilities are large too. However, we expect that ionic polarizabilities contribute to the lattice-dynamical properties only through higher-order terms, although they have a major influence on the Raman-scattering intensities. The properties change gradually from  $\text{K}^+$  to  $\text{Cs}^+$ . However, this does not necessarily mean that the vibrational spectra of the three crystals follow the same pattern and change gradually from  $\text{K}_2\text{SO}_4$  to  $\text{Cs}_2\text{SO}_4$ , because the vibrational spectra are not simply related to the properties of the alkali-metal ions. Changing from  $\text{K}^+$  to  $\text{Rb}^+$  can result in such large changes that some features of the two vibrational spectra no longer correspond. This can be seen from

Figs. 2–4. However, some similarities in the spectra and a consistent variation from  $\text{K}_2\text{SO}_4$  to  $\text{Cs}_2\text{SO}_4$  in both the crystal structures and vibrational frequencies do exist. For example, correspondence between the lowest  $A_g$  vibrational modes and correspondences between internal modes of the three crystals can be found. The reason for the latter is that the influence of the crystal environment on the vibrational properties of the  $\text{SO}_4^{2-}$  group is relatively small.

#### A. Crystal structure

It can be seen from Table IV that the lattice constants increase from  $\text{K}_2\text{SO}_4$  to  $\text{Cs}_2\text{SO}_4$ . The fractional coordinates of ions in the crystal unit cells are about the same for all three sulfates. There are some minor variations, and most of them follow a particular order.

The alkali-metal-ion–oxygen-ion Gordon-Kim short-range potentials for the three sulfates are plotted in Fig. 5. In the interior distance range of interest, i.e., around 6 a.u., the difference between the potentials of  $\text{K}_2\text{SO}_4$  and  $\text{Rb}_2\text{SO}_4$  is smaller than that between  $\text{Rb}_2\text{SO}_4$  and  $\text{Cs}_2\text{SO}_4$ . This is consistent with the values of the ionic radii of the three alkali-metal ions in that the difference between the first two is smaller than that between the last two. In the calculation the static relaxation for all three crystals converges rapidly. The calculated crystal structures are very close to the experimental ones, as seen in Table IV. The calculated lattice constants are smaller than the experimental values for all three crystals, but the errors are within a few percent. The calculated ion fractional coordinates in the crystal unit cells are very close to the experimental values. These results indicate that Gordon-Kim potentials describe well the structural properties of these ionic crystals. The starting point of the static relaxation process was the experimental crystal structure, except for  $\text{Rb}_2\text{SO}_4$ . When the experimental crystal structure was used, the relaxed structure gave several negative frequencies. When the experimental structure of  $\text{Cs}_2\text{SO}_4$

TABLE IV. Lattice parameters of *Pnam* alkali-metal sulfates (in a.u.).

Parameter	$\text{K}_2\text{SO}_4$		$\text{Rb}_2\text{SO}_4$		$\text{Cs}_2\text{SO}_4$	
	Expt.	Calc.	Expt.	Calc.	Expt.	Calc.
$a$	14.1450	13.3850	14.7630	13.9940	15.5690	14.7700
$b$	19.0240	18.2390	19.7010	19.0040	20.6800	19.9040
$c$	10.8210	10.533	11.2800	10.9590	11.8250	11.4550
$x/a$ of S(1)	0.2315	0.2330	0.2380	0.2342	0.241	0.2381
$y/b$ of S(1)	0.4208	0.4195	0.4191	0.4191	0.4172	0.4181
$x/a$ of $M(1,1)$	0.1755	0.1683	0.1750	0.1730	0.1771	0.1766
$y/b$ of $M(1,1)$	0.0884	0.0882	0.0903	0.0884	0.0907	0.0897
$x/a$ of $M(2,1)$	0.9906	0.9897	0.9884	0.9899	0.9888	0.9892
$y/b$ of $M(2,1)$	0.7052	0.7008	0.7030	0.7034	0.7015	0.7026
$x/a$ of O(2,1)	0.2899	0.3100	0.2974	0.3067	0.2973	0.3032
$y/b$ of O(2,1)	0.5576	0.5613	0.5532	0.5557	0.5460	0.5497
$x/a$ of O(3,1)	0.0454	0.0258	0.0471	0.0358	0.0620	0.0498
$y/b$ of O(3,1)	0.4157	0.4227	0.4137	0.4214	0.4127	0.4179
$x/a$ of O(1,1)	0.2996	0.3010	0.3030	0.2996	0.3035	0.3011
$y/b$ of O(1,1)	0.3530	0.3468	0.3540	0.3494	0.3558	0.3523
$z/c$ of O(1,1)	0.0426	0.0348	0.0497	0.0428	0.0570	0.0514

TABLE V. Ionic properties of  $K^+$ ,  $Rb^+$ , and  $Cs^+$ .

Property	$K^+$	$Rb^+$	$Cs^+$
Mass	39.10	85.47	132.91
Electronegativity	0.91	0.89	0.86
Ionic radius $A$	1.33	1.48	1.69
Polarizability	0.84	1.41	2.42

was used instead, the negative frequencies disappeared. This may indicate that the potential surfaces of the alkali-metal sulfates are very flat so that the relaxation process may easily converge on saddle points on the surface. Consequently, the calculation results for  $Rb_2SO_4$  reported here were obtained using the experimental structure of  $Cs_2SO_4$  as the starting point for the relaxation process.

### B. Raman spectra

As mentioned earlier, generally no obviously similar pattern can be found for the external-mode region among the Raman spectra of the three sulfates, especially in the spectral intensities. Since all the modes are identified for the  $A_g$ ,  $B_{2g}$ , and  $B_{3g}$  symmetry, it is possible to make comparisons for these modes. In general, the Raman frequencies decrease from  $K_2SO_4$  to  $Cs_2SO_4$ , and the changes are much larger for the external modes than for the internal modes. The internal modes of the three sulfates correlate well, and the changes follow a simple pattern. It can also be seen that the relative order of the Raman frequency values of different symmetries may change from one crystal to another. The decrease of vibrational frequencies from  $K_2SO_4$  to  $Cs_2SO_4$  is expected. It can be explained by the values of the ionic radii and the masses of the alkali-metal ions. For larger ionic radius, the separations between ions are larger and the Coulomb interactions between ions are smaller. Also, since the vibrational frequency of a harmonic oscillator is proportional to the reciprocal of the square root of the mass, larger values of masses of the ions should result in smaller vibrational frequencies.

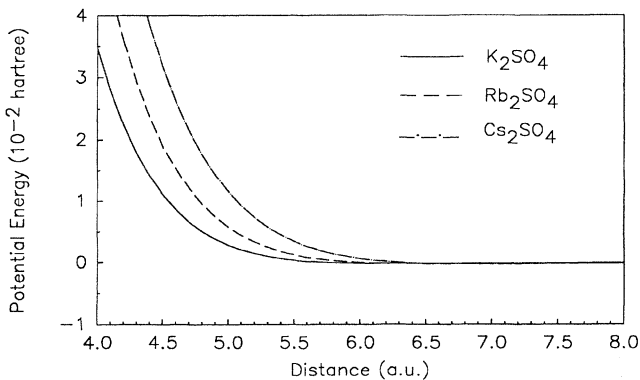


FIG. 5. Gordon-Kim potentials between alkali-metal ions and the oxygen ion.

The intensities of the external modes of the Raman spectra increase from  $K_2SO_4$  to  $Cs_2SO_4$ . For example, the lowest  $A_g$  mode has an intensity of 600 counts for  $K_2SO_4$ , 10 000 for  $Rb_2SO_4$ , and 22 000 for  $Cs_2SO_4$ . Apparently, this is related to the larger polarizabilities of the inner-shell electron distributions of  $Rb^+$  and  $Cs^+$  ions.

It can be seen from Tables I–III that the calculated Raman frequencies, especially those of the external modes, are in general agreement with the experimental values. The agreement seems better for rubidium sulfate and cesium sulfate than for potassium sulfate. The calculated frequencies are higher than the experimental ones for  $K_2SO_4$  for the higher external-mode frequencies. This may be because the Gordon-Kim potentials for the  $K^+$  ion might be a little too hard. The calculated internal frequencies for all three crystals are higher than the experimental values. The principal cause is that zero-point motion for these high frequencies is sufficient to ensure that the effective curvature of the potential for the oxygen motion is significantly smaller than that calculated by GAUSSIAN86.

Common to the  $A_g$  Raman spectra for all three alkali-metal sulfates is a feature at about  $900\text{ cm}^{-1}$ , shown in Fig. 6. It is strongest in the spectrum of cesium sulfate. This feature has a sharp rise and fall with a broad, relatively structureless, nearly flat top, differing from usual first-order Raman peaks. Its spectral shape and temperature independence suggest that it is not due to higher-order Raman scattering either. It is too strong to be attributed to an impurity, because of the relatively high purity of the growth materials. This feature has not been reported for other sulfate crystals and seems peculiar to the  $\beta$ - $K_2SO_4$  structure sulfates. At this time we have not identified the origin of this feature.

Isotope peaks of the totally symmetric internal mode

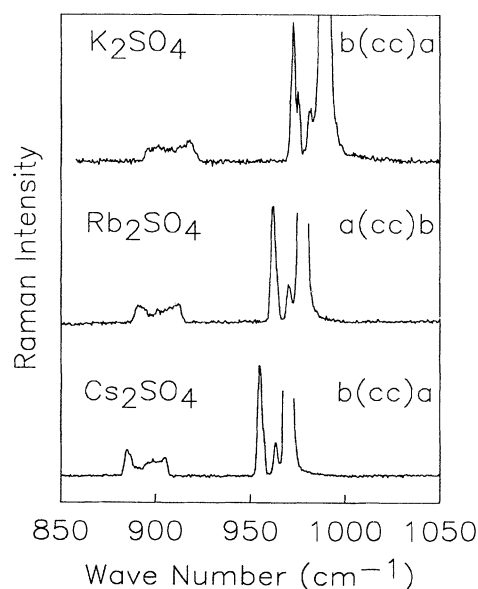


FIG. 6. Isotope peaks of the  $A_g$  internal modes.

be identified for all three alkali-metal sulfates, as shown in Fig. 6. This agrees with the results of Montero, Schmolz, and Haussuhl. They gave a full explanation of these peaks, attributing them to the isotopes  $O^{17}$  and  $O^{18}$  occupying three nonequivalent positions in the sulfate ion. The weaker peak closer to the  $A_g$  peak is attributed to  $O^{17}$ , and the stronger one is attributed to  $O^{18}$ . The triplet structure of the  $O^{18}$  peak can be identified. It can be noted that the separation between the isotope modes becomes smaller from potassium sulfate to cesium sulfate. This indicates that the interaction between the sulfate ion and the alkali-metal ions becomes smaller for cesium sulfate.

#### V. SUMMARY

The Raman spectra of  $K_2SO_4$ ,  $Rb_2SO_4$ , and  $Cs_2SO_4$  were measured at both room and liquid-nitrogen temper-

atures. It was found that there is no straightforward correspondence among the external modes of the Raman spectra of the three sulfate crystals. A particular feature is found at about  $900\text{ cm}^{-1}$  in the  $A_g$  Raman spectra of all three crystals. Its origin remains unexplained.

The crystal structure and the vibrational frequencies of the three sulfate crystals were calculated using a recently extended Gordon-Kim method for the short-range potentials. The calculated crystal structures agree well with the experimental ones. The calculated Raman frequencies are in general agreement with experiment.

#### ACKNOWLEDGMENT

This work was supported by the Army Research Office.

---

<sup>1</sup>M. Gaultier and G. Pannetier, *Bull. Soc. Chim. Fr.* 105 (1968).

<sup>2</sup>K. Gesi, Y. Tominaga, and H. Urabe, *Ferroelect. Lett.* **44**, 71 (1982).

<sup>3</sup>M. Debeau, *Rev. Phys. Appl.* **7**, 49 (1972).

<sup>4</sup>P. Venkateswarlu and H. Broida, *Proc. Indian Acad. Sci. A* **47**, 230 (1971).

<sup>5</sup>S. Montero, R. Schmolz, and S. Haussuhl, *J. Raman Spectrosc.* **2**, 101 (1974).

<sup>6</sup>M. Scrocco, *Phys. Status Solidi B* **91**, K21 (1979).

<sup>7</sup>H. M. Lu and J. R. Hardy, *Phys. Rev. Lett.* **64**, 661 (1990).

<sup>8</sup>D. Liu, H. M. Lu, F. G. Ullman, and J. R. Hardy, *Phys. Rev. B* **43**, 6202 (1991).

<sup>9</sup>M. J. Frisch *et al.*, GAUSSIAN86 (Carnegie-Mellon Quantum Chemistry Publishing Unit, Pittsburgh, PA, 1984).

<sup>10</sup>E. Clementi and C. Roetti, *At. Data Nucl. Data Tables* **12**, 177 (1974).

<sup>11</sup>D. A. Liberman, D. T. Cromer, and J. T. Waber, *Comput. Phys. Commun.* **2**, 107 (1971).